The Unique Paradigm of Spirochete Motility and Chemotaxis

Nyles W. Charon,[1] Andrew Cockburn,[1] Chunhao Li,[3] Jun Liu,[4] Kelly A. Miller,[1] Michael R. Miller,[2] Md. A. Motaleb,[5] and Charles W. Wolgemuth[6]

[1]Department of Microbiology, Immunology, and Cell Biology, [2]Department of Biochemistry, West Virginia University, Health Sciences Center, Morgantown, West Virginia 26506-9177; email: ncharon@hsc.wvu.edu, acockbur@mail.wvu.edu, kamiller@hsc.wvu.edu, mmiller@hsc.wvu.edu

[3]Department of Oral Biology, The State University of New York at Buffalo, New York 14214-3092; email: cli9@buffalo.edu

[4]The University of Texas–Houston Medical School, Department of Pathology and Laboratory Medicine, Houston, Texas 77030; email: jun.liu.1@uth.tmc.edu

[5]Department of Microbiology and Immunology, Brody School of Medicine, East Carolina University, Greenville, North Carolina 27834; email: motalebm@ecu.edu

[6]Department of Cell Biology and Center for Cell Analysis and Modeling, University of Connecticut Health Center, Farmington, Connecticut 06030-3505; email: cwolgemuth@uchc.edu

Annu. Rev. Microbiol. 2012. 66:349–70

The *Annual Review of Microbiology* is online at micro.annualreviews.org

This article's doi: 10.1146/annurev-micro-092611-150145

0066-4227/12/1013-0349$20.00

Keywords

Borrelia, Lyme disease, motor, flagella

Abstract

Spirochete motility is enigmatic: It differs from the motility of most other bacteria in that the entire bacterium is involved in translocation in the absence of external appendages. Using the Lyme disease spirochete *Borrelia burgdorferi* (*Bb*) as a model system, we explore the current research on spirochete motility and chemotaxis. *Bb* has periplasmic flagella (PFs) subterminally attached to each end of the protoplasmic cell cylinder, and surrounding the cell is an outer membrane. These internal helix-shaped PFs allow the spirochete to swim by generating backward-moving waves by rotation. Exciting advances using cryoelectron tomography are presented with respect to in situ analysis of cell, PF, and motor structure. In addition, advances in the dynamics of motility, chemotaxis, gene regulation, and the role of motility and chemotaxis in the life cycle of *Bb* are summarized. The results indicate that the motility paradigms of flagellated bacteria do not apply to these unique bacteria.

Contents

INTRODUCTION

A century ago Clifford Dobell (23) said "the movements of the Spirochaets are still surrounded in mystery." A half century later Claes Weibull (101) quoted Dobell and went on to say "it could be asked whether the situation has changed very much since those days." After yet another half century, although progress has been made, many intriguing questions about spirochete motility remain unanswered and some obscurity about their elegant motions still persists. Genomic analysis indicates that spirochetes are a monophyletic clade (72), so we expect that spirochete motility has some similarity across taxa. Several reviews have been published on spirochete motility and the reader is referred to these articles (15, 34, 51, 102). However, there has been some fresh and robust progress in several areas that focus on particular aspects of spirochete motility, especially on the spirochete *Borrelia burgdorferi* (*Bb*). This progress has been spurred by the increase in research interest in *Bb* because of the importance of the disease it causes and recent breakthroughs in genetic manipulation. Furthermore, owing to its small diameter, *Bb* is optimal for analysis utilizing the groundbreaking methodology of cryoelectron tomography (cryo-ET).

B. burgdorferi Life Cycle, Lyme Disease, and Genomics

Bb: *Borrelia burgdorferi*

Cryo-ET: cryoelectron tomography

Bb is the causative agent of the zoonosis called Lyme disease (81, 86, 89). Small mammals such as mice and voles, and specific species of birds, serve as reservoirs of infection. Humans are accidental hosts. Transmission occurs via the bite of hard shell ticks of certain *Ixodes* species. In humans, Lyme disease has many manifestations, including a spreading rash (erythema migrans), acute and chronic arthritis, a skin disease (acrodermatitis), neurologic problems, and heart block. In the United States, Lyme disease is the most prevalent arthropod-borne human infection. Ten different species in *Bb*

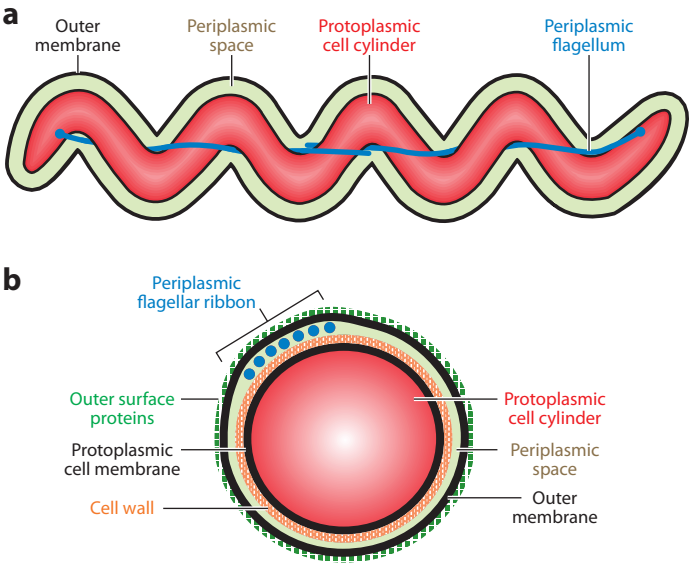

Figure 1

(*a*) Longitudinal diagram of a typical spirochete. Note that the periplasmic flagella overlap in the cell center. (*b*) Cross-section diagram of *Borrelia burgdorferi* illustrating the component parts. Note that seven periplasmic flagella form a tightly packed ribbon that causes the outer membrane to bulge.

have been identified and are called the senso lato species complex. The species that is the most studied is *Bb* senso stricto (hereafter referred to as *Bb*); it is the most prevalent species associated with disease in North America. *Borrelia afzelii* and *Borrelia garinii* are the species most commonly associated with Lyme disease in Eurasia. The genomes of *Bb* senso lato consist of one small, linear chromosome (approximately 950 kb) and a variable number (7–21) of circular and linear plasmids. The plasmids compose approximately one-third of the spirochete's total genetic material. Because of its small genome, *B. burgdorferi* senso lato nutritional requirements is complex.

Structure of a Spirochete

What is a spirochete? In general, spirochetes have a unique and distinct structure; spirochetes are one of the few phyla of bacteria that can be recognized on the basis of morphology (72) (**Figure 1*a***). Outermost is a lipid bilayer outer membrane (OM), and internal to the OM is the protoplasmic cell cylinder (PC). At each end of the PC are subterminally attached periplasmic flagella (PFs) that reside in the periplasmic space (PS). The PFs rotate in a manner similar to the flagella of externally flagellated bacteria (15, 16, 33). The final shape of the cell, depending on the species, is either a helix or a flat wave. The size of the spirochete, the number of PFs attached at each end, and whether the PFs overlap at the middle of the cell vary from species to species. The overall morphology of spirochetes, with their flagella located internally, raises the long-standing questions: How do these bacteria swim and how do they carry out chemotaxis?

OM: outer membrane

PC: protoplasmic cell cylinder

PF: periplasmic flagellum

PS: periplasmic space

TEM: transmission electron microscopy

MORPHOLOGY

B. burgdorferi as a Model Spirochete

Bb fits the morphological description of a spirochete (**Figure 1*b***). Both light-microscopy and high-voltage transmission electron microscopy (TEM) indicate that *Bb* has a flat-wave morphology (32, 33) (**Supplemental Figure 1**, **Supplemental Movie 1**; follow the **Supplemental Material link**

Supplemental Material

from the Annual Reviews home page at **http://www.annualreviews.org**). This planar wave form is similar to that of the syphilis spirochete *Treponema pallidum* (22, 39) but differs from the many helix-shaped members of the phylum such as the family *Leptospiraceae* (72, 77). *Bb* is long and thin, with a length between 10 and 20 μm and a diameter of approximately 300 nm (32). Its shape is characterized as a planar, regular, periodic undulation of the cell body, with an amplitude of 0.78 μm and a wavelength of 2.83 μm.

Ultrastructure of *B. burgdorferi*

The fine structure and general composition of *Bb* have been analyzed using several approaches. The composition of the *Bb* OM is unusual. It lacks lipopolysaccharide but contains lipids uncommon in bacteria, such as cholesterol (8). Cryo-ET has been used extensively to analyze cell structure (17, 43, 54). The OM also has a large number and variety of surface-exposed lipoproteins that are seen by cryo-ET as a layer surrounding the cell (54). The OM has a width of 4 nm and tightly fits around the PC. At the PC surface, the peptidoglycan forms a wall approximately 6.8 nm wide (54). As discussed below, for the spirochete to form a dynamic flat wave and carry out its remarkable motions as it swims, the wall must be astonishingly flexible. Little is known about the structure of the *Bb* peptidoglycan other than that it contains alanine, glycine, glutamic acid, and ornithine (7), and nothing is known about what imparts its highly flexible nature. Inside the wall layer is the 4-nm-wide protoplasmic cell membrane, which encloses the cytoplasm.

Periplasmic Flagella In Situ

Between 7 and 11 PFs are subterminally inserted into each end of the PC (15, 38, 43, 105) (**Figure 1*b*** and **Figure 2**). These PFs are structurally similar to the flagella of other bacteria. Each PF is composed of a motor, hook, and filament. The flagellar motors are linearly inserted along the long axis of the cell at each end and are 90 to 120 nm apart from each other (17, 43, 54, 105). The flagellar motor that is closest to the cell tip is approximately 150 nm from that end. Although previous TEM analyses indicate that the PFs form a bundle (32, 62), recent results with cryo-ET indicate that the flagellar filaments instead form an elegant ribbon in the PS (17) (**Figure 1*b***). The minimum thickness of the ribbon is equivalent to the diameter of a PF

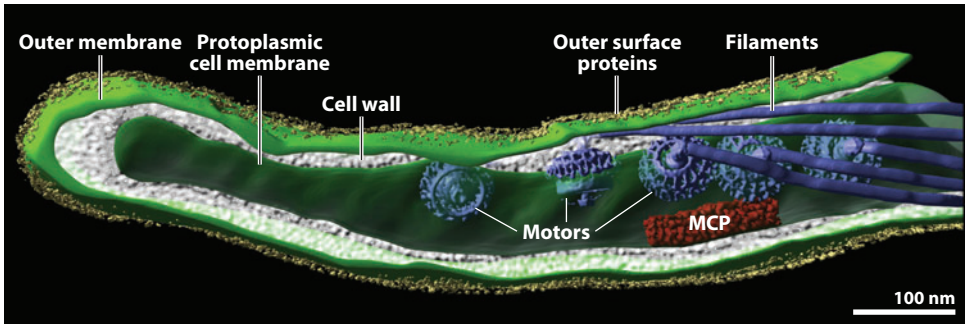

Figure 2

Cellular architecture of one end of *Borrelia burgdorferi* revealed by cryoelectron tomography. A three-dimensional model was generated by manually segmenting the outer membrane, protoplasmic cell membrane, flagellar motors and filaments, methyl-accepting chemotaxis protein (MCP) array, and outer surface proteins. Reprinted and modified with permission from Reference 105.

(16–18 nm) (38, 43), but the ribbon can be thicker and multilayered. The filaments are closely packed, with approximately 3 nm of space between them. The ribbon also increases the thickness of the PS so that the OM bulges in its vicinity (17, 43, 54). Thus, in regions of the cell where there are no PFs, the PS thickness is approximately 16 nm. In contrast, the PS thickness is 42 to 49 nm in domains containing PFs (17, 54). High-voltage TEM and cryo-ET indicate that the ribbons wrap around the body axis (the longitudinal center of the cell, as if the cell is a sausage) clockwise (CW) and thus are right-handed (17, 32). However, along the cell axis (i.e., the abscissa, as the cell is in the form of a flat wave, or a sine wave), the PFs form a left-handed helix with a helix pitch (a complete helical turn) of approximately 2.83 μm, which is equivalent to the periodic wavelength of the cell (32). Recent results suggest that in short cells (10 μm in length) there are more PFs in the cell center than in long cells (20 μm in length) (C. Li, unpublished data). Evidently, the rate of growth of a given flagellar filament decreases as the cells become longer. Furthermore, the two opposing ribbons overlap in the central region. It is not clear whether the two ribbons form a continuous ribbon, or whether the ribbons are on opposite faces of the cell (32, 43, 93).

CW: clockwise

Periplasmic Flagella Structure and Composition

Purified PFs have been analyzed in some detail. At neutral pH, PFs are left-handed and have a helix diameter of 0.28 μm and a pitch of 1.48 μm; however, a small fraction have a helix diameter of 0.8 μm and a pitch of 2.0 μm (16, 24). The flagellar filaments consist of a major 41-kDa FlaB protein and a minor 38-kDa FlaA protein (15, 31). FlaB shows sequence identity to FlaB of other spirochetes and to the flagellar filament proteins of other bacteria such as FliC of *Escherichia coli*. Sequence analysis indicates that FlaB is likely to be excreted into the PS by the Type III flagellin-specific pathway (15). FlaA has sequence identity to FlaA proteins that are present in PFs of other spirochetes. In contrast to FlaB, FlaA is likely to be excreted from the SecA-mediated pathway to the periplasm (15). In most spirochete species, FlaA forms a sheath that surrounds the FlaB core. The function of FlaA is presently unknown, but recent work on the spirochete *Brachyspira hyodysenteriae* is instructive (49). *flaA* mutants of *B. hyodysenteriae* have unsheathed PFs, are still motile, but swim more slowly than the wild type. In addition, the PFs from these mutants have a different helix pitch and diameter and are less rigid than those from the wild type. Thus, FlaA interacts with FlaB to augment filament shape and rigidity for optimal motility. However, in *Bb*, so little FlaA is made relative to FlaB that only a small region of the filament has a sheath (31). TEM analysis comparing the wild type to the *flaA* mutant indicates that the FlaA sheath is localized adjacent to the flagellar hook (S. Shibata, S. Aizawa, M.A. Motaleb & N. Charon, unpublished data). Perhaps flagellar rigidity near this region is essential for optimal PF rotation and motility.

Cytoskeletal Function of the Periplasmic Flagellar Filaments

The analysis of specific mutants indicates that the PFs have a major role in the overall morphology of *Bb*. First, mutants in the following genes form a straight rod instead of a flat wave (**Supplemental Table 1**): *flaB*, which encodes the major flagellin protein; *flgE*, which encodes the flagellar hook; *fliF*, which encodes the MS ring of the motor; and *fliG2*, which encodes a motor protein of the switch complex (50, 62, 84). A mutant that overproduces the regulatory protein CsrA also forms a rod (see below) (93). Ultrastructure and Western blot analyses indicate that the one common deficit of all these mutants is the lack of flagellar filaments and filament proteins. Thus, the ability to form flat waves positively correlates with the presence of flagellar filaments and FlaB. Second, a mutant that has a shorter cellular wavelength and a smaller amplitude than that those of the wild type was recently isolated (93). This mutant, which has a deletion in the *csrA* regulatory gene,

produces PFs that are considerably longer than those of the wild type. Cryo-ET analysis revealed that the flagellar ribbons in *csrA* mutants wrap around the PC more tightly than do ribbons in wild-type cells with a smaller helix pitch and diameter. In addition, the two ribbons interdigitate with one another. These results indicate that increasing the length of the PFs leads to cells with an altered flat-wave morphology (see below). Taken together, the results with the many filament-deficient mutants and the *csrA* deletion mutant strongly support the concept that the PFs influence cell shape by having a skeletal function.

Why is *B. burgdorferi* a Flat Wave?

How do the PFs exert their skeletal function? Bacterial cells and flagella are elastic materials. When forces are applied these structures deform, and when the forces are removed these structures revert back to their original shape. Because the PC of *Bb* is a straight rod when the PFs are not present, and purified PFs are helical, evidently the interaction between the two components leads to the flat-wave morphology. The helix pitch of the PFs in situ (2.83 μm) is markedly different from those that are purified away from the cell body (1.43 μm and 2.0 μm) (16, 24, 32). For the PFs to be contained within the PS, these structures must deform. The PC produces the force that bends the PFs. Concomitantly, the PFs exert an equal but opposite force back onto the PC, which causes the cell to bend into its characteristic shape. Mathematical modeling, which takes into consideration the elastic properties of the PFs and PC, has shown that the balance between these two forces is a cell with a flat-wave shape—it is not intuitive! However, this force balance conspires to produce the correct wavelength and amplitude only if the PFs are in the helical conformation that is observed less frequently in purified PFs (helix diameter of 0.8 μm and a pitch of 2.0 μm) (24). How does the *csrA* deletion mutant that has longer PFs cause the cell to have a shorter wavelength and cell amplitude (93)? One possible explanation is that the increase in length of the PFs, and perhaps the interdigitation characteristic of the PF ribbons in the mutant, causes the PFs to flip into the helical state that is observed more frequently in purified PFs. This change in preferred conformation of the PFs is predicted to produce a flat-wave shape with a smaller wavelength and amplitude.

Hook and Motor Structure

The flagellar hook region in *Bb* and certain other spirochetes has some unique attributes. In other bacteria, the hook serves as a universal joint connecting the flagellar filament to the motor (85). In *Bb*, the hook is a 61-nm-long hollow tube consisting of approximately 133 FlgE units (84). As mentioned above, inactivation of *flgE* results in cells that lack flagellar filaments, are nonmotile, and are rod shaped (84). In most bacteria, the FlgE subunits are held together by protein-protein interactions that are readily dissociated by denaturing agents. Surprisingly, FlgE in *Bb* and other spirochetes forms a stable, high-molecular-weight complex (52, 84). Several lines of evidence indicate that FlgE subunits in *Bb* are covalently cross-linked (84) (K. Miller, M. Miller & N. Charon, unpublished data). The flagellar hook and filament are likely to be under greater stress in spirochetes than in other bacteria, as the PFs deform the PC while they rotate (see below, Dynamics of Motility). Perhaps the hook proteins are cross-linked in spirochetes for added structural strength to perform this function.

The incredible methodology of cryo-ET is being exploited to analyze the intact *Bb* motor (44, 54), as well as other spirochetal motors (53, 69). The overall structures of spirochetal motors are similar to each other, consisting of the MS ring, the C ring, the rod, the export apparatus, and the stator (**Figure 3**) (**Supplemental Movie 2**). *Bb* exhibits a relatively large C ring, ~57 nm in diameter, compared to the 45-nm C ring of *E. coli* and *Salmonella enterica* serovar Typhimurium

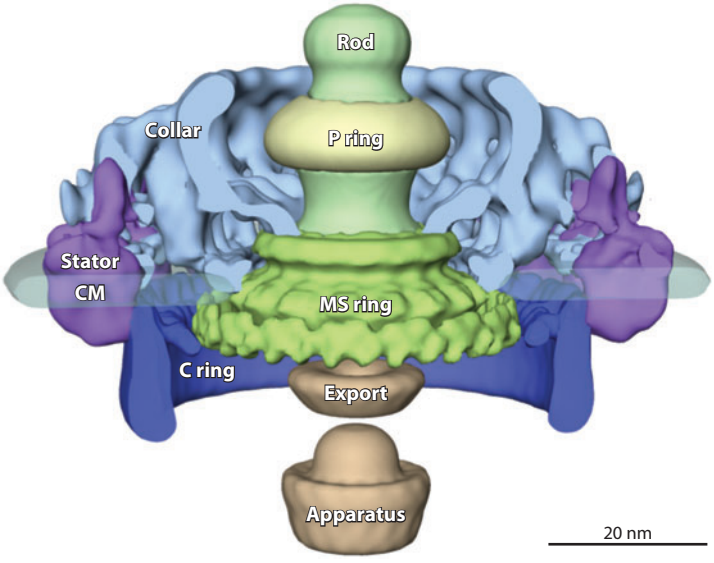

Figure 3

A three-dimensional reconstruction of the *Borrelia burgdorferi* flagellar motor. The major components (the rod, the stator, the P ring, and the MS ring) are labeled. The C ring is composed of FliG, FliM, and FliN. The "collar" is a spirochete-specific feature. The export apparatus is divided into two separate densities, although the boundary between the MS ring and the export apparatus is not well defined. Abbreviation: CM, protoplasmic cell membrane.

(95). This enlarged C ring shares similar features with the *S. enterica* structure: a cylindrical structure with a slightly bulky bottom and a Y-shaped extension at the top (95). Thus, the C ring is likely composed of multiple copies of FliG, FliM, and FliN proteins arranged in a manner similar to that of *E. coli* and *S. enterica*.

The stator, encoded by the *motA* and *motB* genes, is the motor force generator embedded in the protoplasmic cell membrane. The visualization of the stators in many species of bacteria is difficult (19), and this difficulty may in part be the result of the stator being dynamic and that its functional units freely interchange between the motors circulating in the protoplasmic cell membrane (46). In contrast, the stators of *Bb* and other spirochetes are clearly visualized (44, 53, 54, 69). Cryo-ET analysis of *motA* and *motB* mutants of *Bb* provides the first structural evidence that these genes encode the 16 stators radially arranged around the rotor (**Figure 3**) (**Supplemental Movie 2**) (X. Zhao, T. Boquoi, M.A. Motaleb & J. Liu, unpublished data). Conceivably, the stators in *Bb* and other spirochetes are relatively stable, or unit interchange occurs without disrupting the overall arrangement of the stator. Remarkably, the cytoplasmic domain of the stator is adjacent to the C-terminal domain of the C-ring rotor protein FliG. This stator-rotor interaction evidently induces an unexpected conformational change in FliG, and this change is likely to be a fundamental mechanism for flagellar rotation (X. Zhao, T. Boquoi, M.A. Motaleb & J. Liu, unpublished data).

Supplemental Material

The *Bb* flagellar motor is a remarkable and complicated nanomachine consisting of at least 20 different proteins (**Figure 3**) (**Supplemental Movie 2**). To understand flagellar motor assembly and function, the structural and functional roles of all flagellar proteins must be determined. Fortunately, many mutants in motor genes have been constructed by either transposon mutagenesis or targeted mutagenesis (**Supplemental Figure 2**, **Supplemental Table 1**). *fliE* mutants are defective in rod assembly, and *fliM* mutants are deficient in the middle and the bottom of the C ring (X. Zhao, T. Boquoi, A. Manne, M.A. Motaleb & J. Liu, unpublished data). *fliI* and

fliH mutants are defective in the assembly of the bottom part of the export apparatus (X. Zhao, T. Lin & S. Norris, unpublished data). FliL proteins localize between the stator and rotor, and these proteins are evidently involved in the proper orientation of the PFs within the PS (65). *flgI* mutants fail to form a hollow, torus-shaped structure around the rod. However, in contrast to other bacteria, these *flgI* mutants are still fully motile; evidently, the P ring is not required for flagellar rotation (54). Instead, a spirochete-specific "collar" may function as a bushing that facilitates the rotation of the flagellum without disrupting the surrounding peptidoglycan layer. The identities of the specific genes encoding the "collar" have yet to be identified. In sum, the structure of the *Bb* flagellar motor is being characterized in some detail, and specific motor proteins and function are being correlated with specific genes in situ for the first time.

CCW: counterclockwise

DYNAMICS OF MOTILITY

Swimming In Vitro

Given the structure of *Bb*, the obvious first question with respect to their motility is, What do swimming cells look like? Also, given that the PFs are located in the PS, how does PF rotation drive motility? The swimming behavior of *Bb* is more complicated than that of other bacteria as a result of their complex geometry. *Bb* has four motility modes based on the direction of flagellar rotation: two translational modes (with either end leading) and two nontranslational modes (**Figure 4**) (**Supplemental Movie 3**). In an isotropic environment, a given cell runs at least 90% of the time (M.A. Motaleb & N. Charon, unpublished data). During a run, waves are propagated from the front to the back at a frequency of 5 to10 Hz at room temperature. In contrast to eukaryotic flagella, propagating waves are full size at the anterior end instead of starting as small bends and increasing in size. These waves propagate at a speed of 34 $\mu m\ s^{-1}$ relative to the cell (33). The cells swim at a mean speed of 4.25 $\mu m\ s^{-1}$ in a pure liquid (33). The ratio of the swim speed to wave propagation is 0.12; i.e., in the time it takes a wave to travel the length of the cell, the cell advances 12% of its length through the medium. Thus, as *Bb* swims, waves are clearly evident as they swim in a given direction.

How are the waves generated, and what is the basis for the nontranslational forms? Everything points to the PFs. We know they are essential for motility, they rotate, they are helix shaped, and they have a skeletal function. Although it has not been directly proven, the following model is proposed (**Supplemental Movie 4**) (15, 32): During a run, the PFs of the anterior ribbon are predicted to rotate counterclockwise (CCW), and those of the posterior ribbon rotate in the CW direction (as a frame of reference, the PFs are viewed from their distal end to where they insert into the PC). Thus, the PFs of the two ribbons rotate asymmetrically relative to one another during a run. This rotation causes backward-moving waves to be propagated down the length of the cell. Reversals occur when the PFs of both ribbons change the direction of rotation. In addition, recent mathematical modeling suggests that during translation the rotating PFs are not in direct contact with the PC, but rather a thin layer of fluid separates these filaments from the PC (107). Forces between the PFs and the PC are therefore mediated by viscous forces in the fluid present in the PS. This hypothesis is based on the known elasticity of the PFs, PC, and the dynamics of swimming cells. The modeling predicts that the thin layer of fluid in the PS is essential for the smooth backward-propagating waves noted on translating cells. Otherwise, if the PFs interacted directly with the PC, the PFs would be predicted to easily tangle up with one another and the propagating wave would not be as regular as observed. Several questions arise with the overall model of translating *Bb*. If the PFs are rotating CCW along the axis of the cell as viewed from behind the cell, is the cell rolling about the body axis CW to balance that torque as predicted

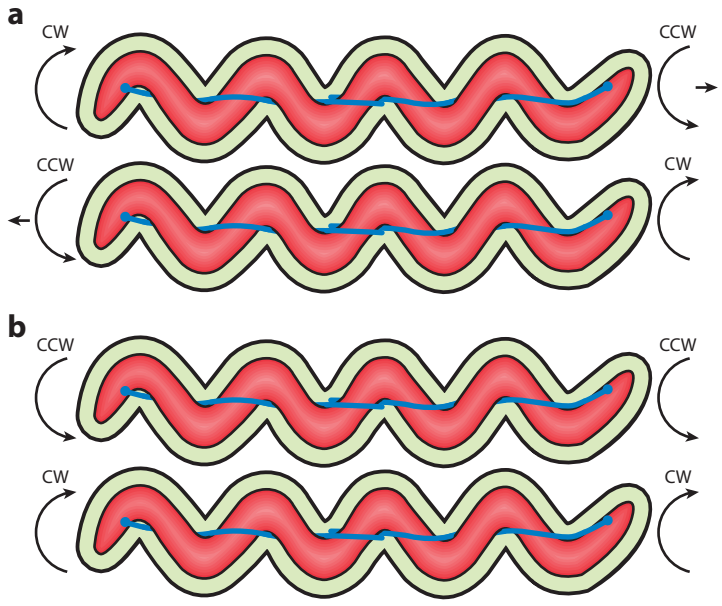

Figure 4

Swimming cells of *Borrelia burgdorferi* as a function of the direction in which the periplasmic flagella (PFs) rotate. Straight arrows at cell ends indicate direction of swimming. Curved arrows indicate the direction in which the PFs rotate. For simplification, only one PF is shown attached at each end of protoplasmic cell cylinder. Panel *a* shows translational forms, and panel *b* shows nontranslational forms. Reprinted and modified with permission from Reference 15. Abbreviations: CW, clockwise; CCW, counterclockwise.

(15, 32)? What is happening to the OM? Cryo-ET indicates that it is held very close to the PC and even bulges in the vicinity of the PF ribbon. How is the tight fitting achieved, especially in light of evidence that the OM is a lipid bilayer? Are there bonds that form between the OM and PC, and are those bonds broken as the PFs rotate?

In the nontranslational modes, the prediction is that the PFs from both ribbons rotate in the same direction: both rotate either CW or CCW. This stopped interval is referred to as a flex and is thought to be analogous to the tumble seen in externally flagellated bacteria. The cells often become distorted during this interval and may bend in the middle. It is difficult to distinguish cells with PFs at both ends rotating CCW from cells with PFs at both ends rotating CW. It is not clear exactly what is occurring in the PS that causes the cell to form a distorted morphology. Do the PFs from the opposite end wind around one another to cause the distorted shape? In other spirochete species, the distortion associated with flexing occurs only if the PFs overlap in the center of the cell (33), so this is a possibility.

The description of swimming given above comes largely from motility assays in liquid environments. Many of the natural environments that *Bb* encounters do not behave like a liquid. For example, spirochetes are deposited into the dermis of the mammal via the saliva of the tick. The dermis of the mammal is composed largely of a cross-linked collagen network. This gel-like environment responds to external forces from the bacterium with a combination of elastic and viscous forces; i.e., it is a viscoelastic material. Liquid media, on the other hand, only responds with viscous forces. One of the first investigations into the effect of viscoelasticity on the motility of *Bb* examined swimming in solutions of methylcellulose or hyaluronic acid (41). Swimming speed increases

GFP: green fluorescent protein

substantially as the concentration of methylcellulose or hyaluronic acid is increased. The increase in swimming speed with the viscoelasticity of the environment suggested that *Bb* motility may be optimized for migration through host tissue. In addition, *Bb*, like several other spirochete species, can translate in highly viscoelastic medium that markedly slows or stops the motility of other flagellated bacteria. Liquid media and methylcellulose solutions, though, are poor facsimiles for many of the natural environments that *Bb* encounters. For example, collagen in the dermis forms a gel-like network (i.e., it is more elastic than viscous), whereas low-concentration methylcellulose solutions (less than a few percent) are viscoelastic fluids (i.e., they are more viscous than elastic) (12). The natural environments are differentiated further from liquid media and methylcellulose solutions because they contain cells and various extracellular matrix components, such as collagen, fibronectin, and decorin, to which *Bb* binds.

Bb in gelatin exhibited four motility states, which are determined by transient adhesion between the bacterium and the matrix (36). In addition to adhering to these substrates, spirochetes also migrate through the matrix, even though the pores in the gelatin matrices are significantly smaller than the diameter of the bacteria. As in previous reports, the undulation and migration speed of the bacteria depend strongly on the physical properties of the environment; however, the bacteria always swim slower in gelatin than in liquid media. Therefore, the unique motility mechanism of *Bb* enables it to penetrate dense tissues in its hosts, but the speed of the bacteria may not be enhanced in these natural environments.

Swimming In Vivo

We are at an early stage in sorting out the role of *Bb* motility in vivo. One of the major breakthroughs is the ability to track green fluorescent protein (GFP)-tagged virulent *Bb* in vivo using intravital microscopy and fluorescence spinning disc confocal microscopy. Soon after injection of *Bb* into mice, spirochetes are seen interacting with capillaries and veins (61). The movement of the organisms is stop and go, with the stops characterized by adherence to the endothelium. Approximately 90% of interactions with the endothelium are less than 1 s, and about 10% are 1–20 s. These interactions are mediated in part by the spirochete surface protein BBK32 and host fibronectin and glycosaminoglycans (70). In contrast, approximately 1% of the cells are stationary, with one end attached and partially embedded in the endothelium, often at the endothelial cell junctures, and the other end gyrating. These stationary cells resemble the often seen tethered spirochetes whereby the cells adhere to stationary ligands via an OM surface-associated component yet remain motile (18). The attached spirochetes eventually escape the endothelial cell lining and penetrate into connective tissue. In the liver, the spirochetes first interact with Kupffer cells, which then trap, immobilize, and engulf the spirochetes, and then present antigens to the invariant natural killer T cells (47). The role of motility and chemotaxis in both the adherence and penetration through blood vessels, and in the interaction of immune cells in the liver, is likely to be important. Future experiments with specific motility and chemotaxis mutants should be definitive.

Some remarkable imaging studies have examined GFP-tagged *Bb* in the tick host both before and after feeding on mice (26). In unfed nymphs, *Bb* cells are nonmotile and distributed throughout the midgut. By 72 h after feeding on mice, the density of *Bb* is high; however, the spirochetes remain nonmotile but are viable. Remarkably, the presence of a diffusible factor(s) in the tick midgut is likely to be responsible for their nonmotility. At 72 h, only a small number of the spirochetes traverse the midgut basement membrane, enter the hemocoel, and colonize the salivary glands for transmission to mammals. These invasive spirochetes are motile. Why is *Bb* motility specifically inhibited in the tick midgut? Perhaps the tick developed a means of defense to keep the infection

localized by inhibiting *Bb* motility. Future experiments to characterize the inhibitory factors should be enlightening.

CHEMOTAXIS

MCP: methyl-accepting chemotaxis protein

Chemotaxis (movement toward or away from a chemical stimulus) in spirochetes is unique. Bacteria undergo a biased random walk during chemotaxis, and this walk is achieved by modulating the direction or speed of flagellar rotation (76, 88, 99). A two-component regulatory system mediates the biased walk up a gradient of attractant or away from a repellent. In the paradigmatic chemotaxis model of *E. coli* and *S. enterica*, variation in motor direction is determined as follows: The response regulator CheY is phosphorylated by the histidine kinase CheA to form CheY-P. CheA is part of the polarly located methyl-accepting chemotaxis protein (MCP) receptor signal complexes. The probability that CheA phosphorylates CheY is a function of the occupancy level of an attractant or repellent that binds directly or indirectly to the MCPs in the PS. CheY-P diffuses through the cytoplasm and interacts with the flagellar switch protein FliM, causing the motor rotational biases to shift from the default rotation of CCW to CW. If all the motors rotate CCW, the cell swims. If one of the motors rotates CW, the cell tumbles (97). The motors are within 1 μm of the MCP complexes. Thus, CheY-P can diffuse and bind to the motors within 0.1 s (98). The CheY-P formed has phosphatase activity associated with it. However, dephosphorylation of CheY-P, which restores the default CCW behavior such that the cell can immediately respond to changes in the environment, is enhanced by the action of the CheY-P-specific phosphatase CheZ.

Chemotaxis in *Bb* is different from this and other well-studied bacterial chemotaxis models. Two conundrums are evident. First, these spirochetes have two sets of flagellar motors: one at each cell end. As noted above, these sets of motors are located at a considerable distance from one another (between 10 and 20 μm). In addition, recent results using fluorescent antibodies and cryo-ET indicate that the MCP complexes are subpolarly located at each cell end (105) (**Figure 2**). If CheY-P is formed at one end of the cell at these complexes, it could readily diffuse to the adjacent motors. However, given a cell length of 10 μm, it would take at least 10 s for CheY-P to diffuse to the motors at the other end of the cell (67). Because the speed of these bacteria is at least 4 μm s^{-1} (33), simple diffusion of CheY-P to the opposite end of the cell to coordinate the rotation of the PFs is unlikely. Furthermore, in *Bb*, instead of runs and tumbling, there are four swim configurations based on the direction of flagellar rotation (**Figure 4**), all of which contribute to a higher level of complexity in swim behavior than that of most other bacteria. Thus, the first conundrum is, How does *Bb* coordinate the rotation of the PFs within the ribbons at both cell ends to effect chemotaxis?

Second, for the bacteria to swim in a given direction, the motors at each end must rotate in the opposite direction of those at the other end; i.e., if the PFs in one ribbon rotate CCW, the others rotate CW. This asymmetrical rotation is markedly different from the swimming behavior of *E. coli* and *S. enterica* whereby all the motors rotate in the same direction during translation. Furthermore, as discussed below, in the absence of a functional CheY response regulator, *Bb* constantly runs. Thus, the second conundrum is, What is the basis for asymmetrical rotation of the PFs during translational swimming in the absence of CheY?

Although significant progress has been made in understanding *Bb* chemotaxis, a palpable molecular model putting it all together is still in the developmental stage. To address the above questions, a capillary tube chemotaxis assay was developed using flow cytometry to enumerate cells, and several chemically defined chemoattractants were identified (4, 63). These attractants include *N*-acetylglucosamine, glucosamine, glucosamine dimers, and glutamate. The assay allowed

researchers to test whether specific genes were involved in chemotaxis. *Bb* has multiple copies of chemotaxis genes, including six *mcp* (two lack membrane-spanning regions), two *cheA*, three *cheY*, two *cheB*, two *cheR*, and three *cheW* (29). It has only one CheY-P phosphatase gene commonly found in bacteria, *cheX*, which has an activity similar to that of *cheZ* found in *E. coli* (64, 74). The results of extensive gene targeting analysis indicated that the chemotaxis pathway involves MCPs, CheW3, CheA2, CheY3, and CheX (**Supplemental Figure 2**, **Supplemental Table 1**). Biochemical analysis supports the conclusion that CheA2 readily phosphorylates CheY3 (67) and CheX dephosphorylates CheY3-P (64, 74). Interestingly, the half-life of the CheY3-P is 10 min (67), which is considerably longer than the half-lives of most CheY-P of other bacteria such as *E. coli*, which is a few seconds (37). Most important, because CheY plays such a pivotal role in the chemotaxis of all known species of bacteria, CheY3 is concluded to be the key chemotaxis response regulator in *Bb*.

Supplemental Material

An analysis of the swim behaviors of the chemotaxis mutants may yield a clue to the basis of asymmetrical rotation of the flagellar ribbons during translational motility. Both *cheA2* and *cheY3* mutants constantly run in one direction (48, 67) (**Supplemental Table 1**, **Supplemental Movie 3**). These results are similar to those of other bacteria such as *E. coli* and *S. enterica*; *cheA* and *cheY* mutants in these bacteria also constantly run. However, in *Bb* the motors rotate asymmetrically at one end relative to the other during a run, whereas in *E. coli* all the motors are rotating CCW. Evidently, in the default state, i.e., when no CheY3-P are present, the motors at one cell end are different from those at the other, as they rotate in opposite directions. Perhaps there is a protein that interacts with motors at one cell end such that in the default state the PFs rotate in the opposite direction relative to those at the other end. There is precedent for protein localization of this type, as some bacteria-specific proteins localize at the old cell end and not at the new cell end (6). A candidate protein is FliG1 (50). *Bb* and many other spirochetes have two *fliG* genes encoded in their genomes, *fliG1* and *fliG2* (29, 50). FliG is involved in motor rotation in other bacteria, is essential for flagellar assembly and motility, and plays a major role in determining the direction of motor rotation (55). *fliG2* likely plays this role in *Bb*, as mutants in this gene are nonmotile and lack PFs; FliG2 has all the essential sequence and structural domains common to other bacterial FliGs (50). However, FliG1 lacks some of the essential residues common to FliG of other bacteria. *fliG1* mutants are still motile but are unable to swim in highly viscous media containing methylcellulose; only one of the cell ends is able to gyrate. Interestingly, GFP-tagged FliG1 localizes at only one cell end (50). It will be interesting to determine whether FliG1 is partly responsible for the asymmetrical rotation of the PFs.

The phenotypes of other specific mutants complicate this scenario. The *cheX* mutant constantly flexes (64), which is analogous to the constantly tumbling *cheZ* mutants of *E. coli* (10). A *cheX* mutant is predicted to have a higher CheY3-P concentration than the wild type does. One expectation of the protein localization model is that cells with a high CheY3-P concentration should also run, not flex. For example, those motors that run CW in the default state should reverse and rotate CCW under a high CheY3-P concentration, and those motors that run CCW in the default state should run CW. Perhaps there is another CheY-P phosphatase that has not been identified in *Bb*, and as result, the *cheX* mutant could have an intermediate level of CheY3-P that results in flexing. In *B. subtilis*, FliY and CheC have CheY-P phosphatase activity, but *Bb* lacks homologs to these genes (68).

Bb also has a gene encoding CheD. CheD in other bacteria augments the phosphatase activity of CheC, binds to and deamidates glutamine residues on MCPs, and regulates the activity of CheA kinase. *cheD* mutants in other bacteria have a decreased activity of CheA kinase, leading to lower levels of CheY-P (78). CheD may have a similar function in *Bb*, as a *cheD* mutant has a nonchemotactic, constantly running phenotype, similar to the *cheY3* and *cheA2* mutants that are also expected to decrease CheY3-P concentration (M.A. Motaleb & N. Charon, unpublished

data). However, because CheD in other bacteria has functions in addition to activating the CheA kinase, its role in *Bb* chemotaxis is presently unclear.

The second messenger, 3′,5′-cyclic-diguanosine monophosphate (c-di-GMP), is emerging as a major factor influencing motility and possibly chemotaxis (see Transcriptional and Translational Regulation of Motility and Chemotaxis Genes, below). Certain mutants involved in c-di-GMP synthesis, degradation, and effector binding have aberrant swim behavior, such that some mutants (e.g., *pdeA*) constantly run, whereas others (e.g., *pdeB*) have a high flex rate (90, 91). c-di-GMP and its effector protein bind to the flagellar motor protein in other bacteria and influence the direction and speed of flagellar rotation (9, 21, 27, 73). At this time it is difficult to determine how c-di-GMP influences *Bb* swimming behavior at a molecular level.

c-di-GMP: 3′,-5′-cyclic-diguanosine monophosphate

The results accumulated indicate the following conclusions: First, CheY3 is the major response regulator, and the pathway leading to its phosphorylation and dephosphorylation involves MCPs, CheW3, CheA2, CheX, and possibly CheD. Second, the asymmetrical rotation of the PFs in the default state can best be explained by differences in the motors at each end of the cell, but support for this hypothesis awaits experimental evidence. Third, it is too early to understand the basis of flagellar coordination mediated by CheY3 that results in chemotaxis, although many hypotheses are conceivable. As previously mentioned, diffusion of CheY3-P from one cell end to the other is too slow to coordinate the rotation of the PFs at the distal end. As an alternative, perhaps there is a cytoskeletal structure whereby CheY-P moves rapidly from one end to the other. There is precedence for this possibility: In *Myxococcus xanthus*, the protein AglZ mediates gliding motility by moving from one cell end to the other by way of the MreB cytoskeleton (58). Because completion of this internal cell migration of AglZ is on the order of several minutes, a CheY3 transport system in *Bb* would have to be considerably faster.

Another model possibility for coordinating the PFs at each end relates to a mechanosensing mechanism. Perhaps there is an interaction between the PFs at one end of the cell and those at the other such that rotation of the PFs at one end influences the rotation of the PFs at the other end. This possibility is conceivable, as the PFs in *Bb* overlap in the center of the cell. However, this hypothesis does not apply to all spirochetes, as *Leptospira interrogans* has PFs that are short and do not overlap (102), yet these spirochetes are chemotactic (110) (N. Takahashi & N. Charon, unpublished data). CheY3-P could act at another, unknown site such that the membrane potential is altered when the cell is undergoing chemotaxis, and this change in potential might allow coordination of the PFs (35). Alternatively, perhaps CheY3-P together with c-di-GMP coordinates PF rotation.

Finally, conceivably there is no internal signal that coordinates the motors at both cell ends: Flagellar coordination and chemotaxis are achieved by the attractant binding to either one or both of the MCP clusters at the cell ends. The change in CheY3-P concentration generated by this binding specifically affects the direction of rotation of the motors that are adjacent to those MCPs. For example, if the attractant binds the MCPs at one cell end, it causes the motors only at that end of the cell to change their direction of rotation, and the cell flexes. In contrast, if attractant molecules simultaneously bind to the MCPs at both cell ends, the motors at both ends change directions and the cell runs. In closing, now that specific compounds that serve as attractants are known, and that CheY3 is the functional response regulator, the basis for coordinating PF rotation for chemotaxis can finally be determined.

TRANSCRIPTIONAL AND TRANSLATIONAL REGULATION OF MOTILITY AND CHEMOTAXIS GENES

The genetic map indicating the genes that are involved in motility and chemotaxis is presented in **Supplemental Figure 2**. Most motility genes are present in single copies (except for *fliG*, the

motor control protein). As noted above, there are multiple copies of chemotaxis genes. The analysis of mutants described above indicates that the *Bb* cluster *cheA2-cheW3-cheX-cheY3* is involved in chemotaxis under standard laboratory conditions. This cluster is closely related to chemotaxis gene systems in the other spirochetes and is probably inherited from a common ancestor (15, 48, 103). The other cluster consisting of *cheW2-bb0566-cheA1-cheB2-bb0569-cheY2* may be a recent gene transfer from the *Proteobacteria* (48, 103). The function of this second cluster is not known, but it may be involved in chemotaxis under different environmental conditions.

The regulation of the motility and chemotaxis genes of *Bb* is unique. In other bacteria, there is cascade control of gene regulation of motility gene expression (20). For example, at least 50 genes are involved in the motility and chemotaxis of *E. coli* and *S. enterica*, and these genes fall into three classes (class I, II, and III), which are under the tight regulation of a transcriptional hierarchy. Within this regulatory cascade, the class I master regulator (FlhDC), in conjunction with the housekeeping sigma factor (σ^{70}), directs RNA polymerase to initiate the transcription of the class II genes. Class II genes encode the structural proteins involved in the motor-hook complexes, and two regulatory elements: the flagellum-specific sigma factor FliA (σ^{28}) and the antagonist of FliA (anti-σ^{28}), FlgM. Prior to the completion of the hook assembly, FlgM binds to FliA to prevent premature synthesis of the class III genes encoding the flagellin and the chemotaxis proteins. Upon completion of the hook structure, FlgM is excreted by the flagellum-export apparatus, thereby allowing FliA to initiate the transcription of the class III genes. The last step allows for completion of flagellar assembly and chemotaxis gene expression. In contrast, in silico analysis indicates that no FliA, FlgM, or σ^{28} promoter consensus sequences are present in the genome of *Bb* (15, 29). All the motility and chemotaxis genes identified thus far fall under the regulation of σ^{70} (**Supplemental Figure 2**). These and other results indicate that *Bb* does not employ a transcription cascade to regulate its motility genes. Instead, these genes are regulated primarily by a posttranscriptional mechanism. Two key studies that lead to this conclusion stand out. First, in a *flaB* filament mutant, the amount of FlaA synthesized is only 13% of the wild-type level despite equivalent levels of *flaA* transcript (66). Second, in a *flgE* mutant, FlaA and FlaB accumulation are decreased by more than 80%, whereas the levels of their respective encoding mRNA are equivalent to those of the wild type (84). Furthermore, although FlaA is slowly degraded in the *flgE* mutant, there is no turnover of FlaB. The conclusion is that translational control and not protein turnover is responsible for the lack of accumulation of FlaB and possibly that of FlaA in the *flgE* mutant.

Recent experiments indicate that the *Bb* carbon storage regulator A (CsrA) is a major regulator of translational control of FlaB (93). The Csr system is present in many bacterial species (3, 80), and its importance in carbon metabolism, virulence, biofilm formation, and motility is well established (2, 56, 80). In *E. coli*, the Csr system comprises an RNA binding protein, CsrA; two noncoding RNAs, CsrB and CsrC; and a regulatory protein, CsrD. CsrA functions through binding to the consensus sequence RUACARGGAUGU, which is present within the leader region of its targeted transcripts and subsequently regulates gene expression posttranscriptionally (25, 60). In *E. coli*, CsrA positively regulates flagellar synthesis by serving as an activator of *flhDC* expression (100). However, in *B. subtilis*, CsrA has an opposite effect—it negatively regulates flagellin synthesis at a posttranscriptional level by binding to mRNA and inhibiting translation (106). In a similar manner, *Bb* CsrA is a negative regulator of FlaB. CsrA binds to two sites present in the leader region of the *flaB* transcript, with one of them overlapping the Shine-Dalgarno sequence. Binding of CsrA to these regions leads to translation inhibition of FlaB, presumably via blocking ribosomes from accessing the Shine-Dalgarno sequence of *flaB* mRNA. Thus, the amount of FlaB in a cell may be controlled at the translational level by CsrA (93).

The two-component regulatory system called HK2/Rrp2 is involved in motility gene expression in *Bb* (42, 71, 104). Acetyl-phosphate, an intermediate product from acetate metabolism,

autophosphorylates Rrp2, the response regulator of the HK2/Rrp2, and in doing so activates RpoN, a σ^{54} transcription factor. RpoN in turn upregulates RpoS (the Rrp2-RpoN-RpoS pathway) (104). CsrA serves as a repressor of phosphoacetyltransferase (Pta), one of the key proteins in acetate metabolism, and indirectly modulates the level of acetyl-phosphate in *Bb* as well as the subsequent activation of the Rrp2-RpoN-RpoS pathway (92). Microarray analysis of *rrp2*, *rpoN*, and *rpoS* mutants has revealed a potential role for the Rrp2-RpoN-RpoS network in the regulation of chemotaxis gene expression (14, 28, 71). For instance, the transcription of eight chemotaxis genes is regulated by the Rrp2-RpoN-RpoS network (71). Interestingly, Rrp2-RpoN-RpoS activity is maximally induced under conditions that mimic the mammalian host environment (108). Regulation of chemotaxis proteins via the Rrp2 pathway may allow the spirochete to modulate its chemotaxis genes expression while being transmitted between different hosts to aid in colonization as well as dissemination.

Recent studies in *Bb* indicate a link between the signaling molecule second-messenger c-di-GMP and cell motility (42, 75, 90, 91). In *Bb*, the c-di-GMP metabolism pathway consists of Rrp1, a sole diguanylate cyclase (42, 83); two phosphodiesterases, PdeA and PdeB (90, 91); and PlzA (30, 75), a c-di-GMP binding protein. A mutation in any of the genes of the c-di-GMP pathway alters both cell motility and chemotaxis, but many different phenotypes are generated. For example, disruption of Rrp1 causes cells to constantly run and have an attenuated chemotactic response (42). Mutations in the phosphodiesterase genes result in two different phenotypes: A *pdeA* mutant runs and pauses but fails to reverse, and a *pdeB* mutant has increased flexing frequency (90, 91). A *plzA* mutant has a defect in motility in agar but has the wild-type swimming behavior (75). Remarkably, the *plzApdeB* double mutant constantly flexes (90). Taken together, c-di-GMP clearly affects motor function in *Bb*, but as previously stated, how this occurs is unclear.

In summary, our understating of the regulation of chemotaxis and motility gene expression in *Bb* is still in its infancy. Translational control of motility gene expression appears to be crucial, with CsrA and c-di-GMP emerging as major regulators of chemotaxis and motility. Many questions remain unanswered. What is the interplay between the identified regulatory elements in modulating gene expression? How do environmental cues play a role in differential gene expression within the two hosts, and what are those cues?

VIRULENCE AS RELATED TO CHEMOTAXIS AND MOTILITY

The role of motility and chemotaxis during the infection and disease processes has been examined in several species of pathogenic bacteria. In many species, mutant analysis indicates that motility and chemotaxis are essential for infection and invasion (13, 40, 59, 109). Among the spirochetes, motility-deficient mutants of *Brachyspira hyodysenteriae* are attenuated in a mouse model of swine dysentery (82). In *Treponema denticola*, motility- and chemotaxis-deficient mutants are less invasive than their parent in a human gingival keratinocyte monolayer cell penetration model (57). Recent results suggest that motility is essential for *L. interrogans* to cause disease in the hamster model for leptospirosis (45; E. Wunder & A. Ko, unpublished data).

Motility and chemotaxis are likely to be important factors for *Bb* to survive in nature. Genomic analysis suggests that over 50 genes (5–6% of the genome) are potentially involved in motility and chemotaxis (15, 29). In addition, approximately 10% of the total cellular protein is FlaB (66). These results imply *Bb* dedicates a significant proportion of its energy to motility and chemotaxis, and they further support the concept that these processes are necessary for the survival of the spirochete. In addition, during mammalian infection, and when growing *Bb* under conditions that mimic in vivo conditions, motility and chemotaxis proteins are upregulated and some are among

the most potent immunogens (5, 79, 96). Evidently the synthesis of these proteins is not turned off soon after infection as in some species of bacteria (1).

Motility and chemotaxis are likely to be important for *Bb* to participate in several steps in completing the host-vector cycle. First, after transmission from the tick to a vertebrate host, *Bb* disseminates through skin and migrates to an appropriate target tissue such as the joint. These sites allow for persistence and evasion of the expanding adaptive immune response. Second, after residing in the vertebrate host for weeks to years, *Bb* possibly detects the presence of feeding ticks, and then migrates to those sites to enter the blood meal of those ticks. Finally, during the blood meal of an infected tick, the spirochetes need to migrate from the tick gut to the salivary glands to restart the cycle.

Although using a genetic approach to determine the contribution of motility and chemotaxis to the life cycle of *Bb* is difficult (15, 65), significant progress is being made. One key study focused on the presumed motor protein *fliG1* gene from a virulent strain of *Bb* (11, 50). Mutations in this gene result in motility-deficient cells and are unable to establish an infection in mice. These studies are the first to show that motility is involved in the virulence of *Bb.* In another ongoing study, targeted *flaB* mutants from a virulent strain of *Bb* are nonmotile as expected, but they are also noninfectious in mice (S. Sultan, M.A. Motaleb, P. Stewart, P. Rosa & N. Charon, unpublished data). These preliminary results, coupled with those with the *fliG1* mutant, suggest that motility plays a critical role in the disease process.

Recent results suggest that chemotaxis may also be involved in *Bb* virulence. *Bb* is attracted to tick salivary extract (87). In a recent study, a nonchemotactic *cheA2* mutant failed to infect either immunocompetent or immunodeficient mice and was quickly eliminated from the initial inoculation sites. Furthermore, tick-mouse infection studies revealed that although the mutant was able to survive in ticks, it failed to establish a new infection in mice via tick bites (94). The altered phenotypes were restored when the mutant was complemented. In addition, both a nonchemotactic *cheY3* mutant (M.A. Motaleb, unpublished data) and a c-di-GMP *pdeA* mutant that constantly runs were unable to infect mice (91). Collectively, these data demonstrate that *Bb* needs chemotaxis to establish mammalian infection and to accomplish its natural enzootic cycle. We expect that the analysis of other motility and chemotaxis mutants will lead to a better understanding of these processes with respect to tick transmission and mammalian infection and disease.

CONCLUSION

In this review we summarize the developments made in understanding spirochete motility and chemotaxis with *Bb* chosen as the model. Significant progress has been made since the times of Dobell and Weibull, but many questions still remain. Spirochetes cause dreadful diseases prevalent throughout the world including syphilis, leptospirosis, relapsing fever, and Lyme disease. The tragedy is that so little is known about these terrifying bacteria: We cannot even grow the syphilis spirochete in the laboratory, and only a handful of laboratories in the world are doing basic studies on *Treponema pallidum*. We can only hope that in another half century (or sooner!) sufficient progress in our understanding of the biology of these enigmatic pathogens will lead to new means of disease prevention and treatment such that these diseases are eliminated.

SUMMARY POINTS

1. Cryo-ET allows for exquisitely detailed analysis of the *Bb* flagellar motor.
2. When *Bb* swims in one direction in the absence of the response regulator CheY3-P, it rotates the PFs of the polar ribbons asymmetrically.

3. *Bb* is so long that chemotaxis models as described in other bacteria do not directly apply.
4. *Bb* lacks the cascade control of motility and chemotaxis gene expression and relies on translational control.
5. Initial gene targeting experiments indicate that motility and chemotaxis play important roles in the life cycle of *Bb* in both tick and mammalian hosts.

FUTURE ISSUES

1. What are the functions of each motor protein in generating flagellar rotation?
2. What is the molecular basis for asymmetrical flagellar rotation in the absence of CheY3-P?
3. What is the molecular mechanism of chemotaxis in *Bb* and how is the direction of flagellar rotation controlled?
4. What are the details of motility and chemotaxis gene expression in *Bb*, and how do CsrA and c-di-GMP exert their activities?
5. What are the precise points of involvement of motility and chemotaxis in the life cycle of *Bb*?

DISCLOSURE STATEMENT

The authors are not aware of any affiliations, memberships, funding, or financial holdings that might be perceived as affecting the objectivity of this review.

ACKNOWLEDGMENTS

The authors dedicate this review to Professor Stuart F. Goldstein in honor of his forthcoming retirement from the University of Minnesota. His contributions have been crucial in understanding spirochete motility and in moving the field forward. We appreciate the comments and suggestions by J. Coburn, S. Goldstein, M. James, R. Silversmith, V. Sourjik, and M. Wooten. The research in this review was supported by Public Health Service grants AI078958 to C.L., GM0072004 to C.W., AR060834 to M.A.M., AI29743 and AI093917 to N.W.C. and M.R.M., and AI087946 and a Welch Foundation grant (AU-1714) to J.L. K.A.M. is supported by an American Heart Association graduate fellowship and WVNano.

LITERATURE CITED

1. Akerley BJ, Cotter PA, Miller JF. 1995. Ectopic expression of the flagellar regulon alters development of the *Bordetella*-host interaction. *Cell* 80:611–20
2. Babitzke P, Baker CS, Romeo T. 2009. Regulation of translation initiation by RNA binding proteins. *Annu. Rev. Microbiol.* 63:27–44
3. Babitzke P, Romeo T. 2007. CsrB sRNA family: sequestration of RNA-binding regulatory proteins. *Curr. Opin. Microbiol.* 10:156–63

4. Bakker RG, Li C, Miller MR, Cunningham C, Charon NW. 2007. Identification of specific chemoattractants and genetic complementation of a *Borrelia burgdorferi* chemotaxis mutant: a flow cytometry-based capillary tube chemotaxis assay. *Appl. Environ. Microbiol.* 73:1180–88
5. Barbour AG, Jasinskas A, Kayala MA, Davies DH, Steere AC, et al. 2008. A genome-wide proteome array reveals a limited set of immunogens in natural infections of humans and white-footed mice with *Borrelia burgdorferi*. *Infect. Immun.* 76:3374–89
6. Bardy SL, Maddock JR. 2007. Polar explorations: recent insights into the polarity of bacterial proteins. *Curr. Opin. Microbiol.* 10:617–23
7. Beck G, Benach JL, Habicht GS. 1990. Isolation, preliminary chemical characterization, and biological activity of *Borrelia burgdorferi* peptidoglycan. *Biochem. Biophys. Res. Commun.* 167:89–95
8. Ben-Menachem G, Kubler-Kielb J, Coxon B, Yergey A, Schneerson R. 2003. A newly discovered cholesteryl galactoside from *Borrelia burgdorferi*. *Proc. Natl. Acad. Sci. USA* 100:7913–18
9. Boehm A, Kaiser M, Li H, Spangler C, Kasper CA, et al. 2010. Second messenger-mediated adjustment of bacterial swimming velocity. *Cell* 141:107–16
10. Boesch KC, Silversmith RE, Bourret RB. 2000. Isolation and characterization of nonchemotactic CheZ mutants of *Escherichia coli*. *J. Bacteriol.* 182:3544–52
11. Botkin DJ, Abbott AN, Stewart PE, Rosa PA, Kawabata H, et al. 2006. Identification of potential virulence determinants by Himar1 transposition of infectious *Borrelia burgdorferi* B31. *Infect. Immun.* 74:6690–99
12. Brau RR, Ferrer JM, Lee H, Castro E, Tam BK, et al. 2007. Passive and active microrheology with optical tweezers. *J. Opt. A* 9:S103–12
13. Butler SM, Camilli A. 2005. Going against the grain: chemotaxis and infection in *Vibrio cholerae*. *Nat. Rev. Microbiol.* 3:611–20
14. Caimano MJ, Iyer R, Eggers CH, Gonzalez C, Morton EA, et al. 2007. Analysis of the RpoS regulon in *Borrelia burgdorferi* in response to mammalian host signals provides insight into RpoS function during the enzootic cycle. *Mol. Microbiol.* 65:1193–217

15. Provides a general review of motility and chemotaxis of spirochetes.

15. Charon NW, Goldstein SF. 2002. Genetics of motility and chemotaxis of a fascinating group of bacteria: the spirochetes. *Annu. Rev. Genet.* 36:47–73

16. Charon NW, Goldstein SF, Block SM, Curci K, Ruby JD, et al. 1992. Morphology and dynamics of protruding spirochete periplasmic flagella. *J. Bacteriol.* 174:832–40
17. Charon NW, Goldstein SF, Marko M, Hsieh C, Gebhardt LL, et al. 2009. The flat-ribbon configuration of the periplasmic flagella of *Borrelia burgdorferi* and its relationship to motility and morphology. *J. Bacteriol.* 191:600–7
18. Charon NW, Lawrence CW, O'Brien S. 1981. Movement of antibody-coated latex beads attached to the spirochete *Leptospira interrogans*. *Proc. Natl. Acad. Sci. USA* 78:7166–70
19. Chen S, Beeby M, Murphy GE, Leadbetter JR, Hendrixson DR, et al. 2011. Structural diversity of bacterial flagellar motors. *EMBO J.* 30:2972–81

20. Reviews the control of assembly of the flagellar motor.

20. Chevance FF, Hughes KT. 2008. Coordinating assembly of a bacterial macromolecular machine. *Nat. Rev. Microbiol.* 6:455–65

21. Christen M, Christen B, Allan MG, Folcher M, Jeno P, et al. 2007. DgrA is a member of a new family of cyclic diguanosine monophosphate receptors and controls flagellar motor function in *Caulobacter crescentus*. *Proc. Natl. Acad. Sci. USA* 104:4112–17
22. Cox CD. 1972. Shape of *Treponema pallidum*. *J. Bacteriol.* 109:943–44
23. Dobell C. 1912. Researches on the spirochaets and related organisms. *Arch. Protistenk.* 26:117–239
24. Dombrowski C, Kan W, Motaleb MA, Charon NW, Goldstein RE, Wolgemuth CW. 2009. The elastic basis for the shape of *Borrelia burgdorferi*. *Biophys. J.* 96:4409–17
25. Dubey AK, Baker CS, Romeo T, Babitzke P. 2005. RNA sequence and secondary structure participate in high-affinity CsrA-RNA interaction. *RNA* 11:1579–87
26. Dunham-Ems SM, Caimano MJ, Pal U, Wolgemuth CW, Eggers CH, et al. 2009. Live imaging reveals a biphasic mode of dissemination of *Borrelia burgdorferi* within ticks. *J. Clin. Invest.* 119:3652–65
27. Fang X, Gomelsky M. 2010. A post-translational, c-di-GMP-dependent mechanism regulating flagellar motility. *Mol. Microbiol.* 76:1295–305

28. Fisher MA, Grimm D, Henion AK, Elias AF, Stewart PE, et al. 2005. *Borrelia burgdorferi* sigma^{54} is required for mammalian infection and vector transmission but not for tick colonization. *Proc. Natl. Acad. Sci. USA* 102:5162–67
29. Fraser CM, Casjens S, Huang WM, Sutton GG, Clayton R, et al. 1997. Genomic sequence of a Lyme disease spirochaete, *Borrelia burgdorferi*. *Nature* 390:580–86
30. Freedman JC, Rogers EA, Kostick JL, Zhang H, Iyer R, et al. 2010. Identification and molecular characterization of a cyclic-di-GMP effector protein, PlzA (BB0733): additional evidence for the existence of a functional cyclic-di-GMP regulatory network in the Lyme disease spirochete, *Borrelia burgdorferi*. *FEMS Immunol. Med. Microbiol.* 58:285–94
31. Ge Y, Li C, Corum L, Slaughter CA, Charon NW. 1998. Structure and expression of the FlaA periplasmic flagellar protein of *Borrelia burgdorferi*. *J. Bacteriol.* 180:2418–25
32. Goldstein SF, Buttle KF, Charon NW. 1996. Structural analysis of *Leptospiraceae* and *Borrelia burgdorferi* by high-voltage electron microscopy. *J. Bacteriol.* 178:6539–45
33. Goldstein SF, Charon NW, Kreiling JA. 1994. *Borrelia burgdorferi* swims with a planar waveform similar to that of eukaryotic flagella. *Proc. Natl. Acad. Sci. USA* 91:3433–37
34. Goldstein SF, Li C, Liu J, Miller MR, Motaleb MA, et al. 2010. The chic motility and chemotaxis of *Borrelia burgdorferi*. In *Borrelia: Molecular Biology, Host Interaction, and Pathogenesis*, ed. D Scott Samuels, JD Radolf, pp. 167–87. Norfolk, UK: Calister Acad.
35. Goulbourne EA Jr, Greenberg EP. 1981. Chemotaxis of *Spirochaeta aurantia:* involvement of membrane potential in chemosensory signal transduction. *J. Bacteriol.* 148:837–44
36. Harman MW, Dunham-Ems SM, Caimano MJ, Belperron AA, Bockenstedt LK, et al. 2012. The heterogeneous motility of the Lyme disease spirochete in gelatin mimics dissemination through tissue. *Proc. Natl. Acad. Sci. USA.* 109:3059–64
37. Hess JF, Oosawa K, Kaplan N, Simon MI. 1988. Phosphorylation of three proteins in the signaling pathway of bacterial chemotaxis. *Cell* 53:79–87
38. Hovind-Hougen K. 1984. Ultrastructure of spirochetes isolated from *Ixodes ricinus* and *Ixodes dammini*. *Yale J. Biol. Med.* 57:543–48
39. Izard J, Renken C, Hsieh C, Desrosiers DC, Dunham-Ems S, et al. 2009. Cryo-electron tomography elucidates the molecular architecture of *Treponema pallidum*, the syphilis spirochete. *J. Bacteriol.* 191:7566–80
40. Josenhans C, Suerbaum S. 2002. The role of motility as a virulence factor in bacteria. *Int. J. Med. Microbiol.* 291:605–14
41. Kimsey RB, Spielman A. 1990. Motility of Lyme disease spirochetes in fluids as viscous as the extracellular matrix. *J. Infect. Dis.* 162:1205–8
42. Kostick JL, Szkotnicki LT, Rogers EA, Bocci P, Raffaelli N, Marconi RT. 2011. The diguanylate cyclase, Rrp1, regulates critical steps in the enzootic cycle of the Lyme disease spirochetes. *Mol. Microbiol.* 81:219–31
43. Kudryashev M, Cyrklaff M, Baumeister W, Simon MM, Wallich R, Frischknecht F. 2009. Comparative cryo-electron tomography of pathogenic Lyme disease spirochetes. *Mol. Microbiol.* 71:1415–34
44. Kudryashev M, Cyrklaff M, Wallich R, Baumeister W, Frischknecht F. 2010. Distinct in situ structures of the *Borrelia* flagellar motor. *J. Struct. Biol.* 169:54–61
45. Lambert A, Picardeau M, Haake DA, Sermswan RW, Srikram A, et al. 2012. FlaA proteins in *Leptospira interrogans* are essential for motility and virulence but are not required for formation of the flagellum sheath. *Infect. Immun.* 80:2019–25
46. Leake MC, Chandler JH, Wadhams GH, Bai F, Berry RM, Armitage JP. 2006. Stoichiometry and turnover in single, functioning membrane protein complexes. *Nature* 443:355–58
47. Lee WY, Moriarty TJ, Wong CH, Zhou H, Strieter RM, et al. 2010. An intravascular immune response to *Borrelia burgdorferi* involves Kupffer cells and iNKT cells. *Nat. Immunol.* 11:295–302
48. Li C, Bakker RG, Motaleb MA, Sartakova ML, Cabello FC, Charon NW. 2002. Asymmetrical flagellar rotation in *Borrelia burgdorferi* nonchemotactic mutants. *Proc. Natl. Acad. Sci. USA* 99:6169–74
49. Li C, Wolgemuth CW, Marko M, Morgan DG, Charon NW. 2008. Genetic analysis of spirochete flagellin proteins and their involvement in motility, filament assembly, and flagellar morphology. *J. Bacteriol.* 190:5607–15

50. Li C, Xu H, Zhang K, Liang FT. 2010. Inactivation of a putative flagellar motor switch protein FliG1 prevents *Borrelia burgdorferi* from swimming in highly viscous media and blocks its infectivity. *Mol. Microbiol.* 75:1563–76
51. Limberger RJ. 2004. The periplasmic flagellum of spirochetes. *J. Mol. Microbiol. Biotechnol.* 7:30–40
52. Limberger RJ, Slivienski LL, Samsonoff WA. 1994. Genetic and biochemical analysis of the flagellar hook of *Treponema phagedenis*. *J. Bacteriol.* 176:3631–37
53. Liu J, Howell JK, Bradley SD, Zheng Y, Zhou ZH, Norris SJ. 2010. Cellular architecture of *Treponema pallidum*: novel flagellum, periplasmic cone, and cell envelope as revealed by cryo electron tomography. *J. Mol. Biol.* 403:546–61

54. Detailed examination of the *Bb* motor in situ at a resolution of 3.5 nm using cryo-ET.

54. Liu J, Lin T, Botkin DJ, McCrum E, Winkler H, Norris SJ. 2009. Intact flagellar motor of Borrelia burgdorferi revealed by cryo-electron tomography: evidence for stator ring curvature and rotor/C-ring assembly flexion. *J. Bacteriol.* 191:5026–36

55. Lloyd SA, Tang H, Wang X, Billings S, Blair DF. 1996. Torque generation in the flagellar motor of *Escherichia coli*: evidence of a direct role for FliG but not for FliM or FliN. *J. Bacteriol.* 178:223–31
56. Lucchetti-Miganeh C, Burrowes E, Baysse C, Ermel G. 2008. The post-transcriptional regulator CsrA plays a central role in the adaptation of bacterial pathogens to different stages of infection in animal hosts. *Microbiology* 154:16–29
57. Lux R, Miller JN, Park NH, Shi W. 2001. Motility and chemotaxis in tissue penetration of oral epithelial cell layers by *Treponema denticola*. *Infect. Immun.* 69:6276–83
58. Mauriello EM, Mignot T, Yang Z, Zusman DR. 2010. Gliding motility revisited: How do the myxobacteria move without flagella? *Microbiol. Mol. Biol. Rev.* 74:229–49
59. McGee DJ, Langford ML, Watson EL, Carter JE, Chen YT, Ottemann KM. 2005. Colonization and inflammation deficiencies in Mongolian gerbils infected by *Helicobacter pylori* chemotaxis mutants. *Infect. Immun.* 73:1820–27
60. Mercante J, Edwards AN, Dubey AK, Babitzke P, Romeo T. 2009. Molecular geometry of CsrA (RsmA) binding to RNA and its implications for regulated expression. *J. Mol. Biol.* 392:511–28
61. Moriarty TJ, Norman MU, Colarusso P, Bankhead T, Kubes P, Chaconas G. 2008. Real-time high resolution 3D imaging of the Lyme disease spirochete adhering to and escaping from the vasculature of a living host. *PLoS Pathog.* 4:e1000090
62. Motaleb MA, Corum L, Bono JL, Elias AF, Rosa P, et al. 2000. *Borrelia burgdorferi* periplasmic flagella have both skeletal and motility functions. *Proc. Natl. Acad. Sci. USA* 97:10899–904
63. Motaleb MA, Miller MR, Bakker RG, Li C, Charon NW. 2007. Isolation and characterization of chemotaxis mutants of the Lyme disease spirochete *Borrelia burgdorferi* using allelic exchange mutagenesis, flow cytometry, and cell tracking. *Methods Enzymol.* 422:419–37
64. Motaleb MA, Miller MR, Li C, Bakker RG, Goldstein SF, et al. 2005. CheX is a phosphorylated CheY phosphatase essential for *Borrelia burgdorferi* chemotaxis. *J. Bacteriol.* 187:7963–69
65. Motaleb MA, Pitzer JE, Sultan SZ, Liu J. 2011. A novel gene inactivation system reveals altered periplasmic flagellar orientation in a *Borrelia burgdorferi fliL* mutant. *J. Bacteriol.* 193:3324–31
66. Motaleb MA, Sal MS, Charon NW. 2004. The decrease in FlaA observed in a *flaB* mutant of *Borrelia burgdorferi* occurs posttranscriptionally. *J. Bacteriol.* 186:3703–11
67. Motaleb MA, Sultan SZ, Miller MR, Li C, Charon NW. 2011. CheY3 of *Borrelia burgdorferi* is the key response regulator essential for chemotaxis and forms a long-lived phosphorylated intermediate. *J. Bacteriol.* 193:3332–41
68. Muff TJ, Ordal GW. 2008. The diverse CheC-type phosphatases: chemotaxis and beyond. *Mol. Microbiol.* 70:1054–61

69. First examination of the flagellar motor in situ using cryo-ET.

69. Murphy GE, Leadbetter JR, Jensen GJ. 2006. In situ structure of the complete Treponema primitia flagellar motor. Nature 442:1062–64

70. Norman MU, Moriarty TJ, Dresser AR, Millen B, Kubes P, Chaconas G. 2008. Molecular mechanisms involved in vascular interactions of the Lyme disease pathogen in a living host. *PLoS Pathog.* 4:e1000169
71. Ouyang Z, Blevins JS, Norgard MV. 2008. Transcriptional interplay among the regulators Rrp2, RpoN and RpoS in *Borrelia burgdorferi*. *Microbiology* 154:2641–58

72. Paster BJ. 2011. Phylum XV. Spirochaetes Garrity and Holt 2001. In *Bergey's Manual of Systematic Bacteriology*, ed. NR Krieg, W Ludwig, WB Whitman, BP Hedlund, BJ Paster, et al., 4:471–566. New York: Springer
73. Paul K, Nieto V, Carlquist WC, Blair DF, Harshey RM. 2010. The c-di-GMP binding protein YcgR controls flagellar motor direction and speed to affect chemotaxis by a "backstop brake" mechanism. *Mol. Cell* 38:128–39
74. Pazy Y, Motaleb MA, Guarnieri MT, Charon NW, Zhao R, Silversmith RE. 2010. Identical phosphatase mechanisms achieved through distinct modes of binding phosphoprotein substrate. *Proc. Natl. Acad. Sci. USA* 107:1924–29
75. Pitzer JE, Sultan SZ, Hayakawa Y, Hobbs G, Miller MR, Motaleb MA. 2011. Analysis of the *Borrelia burgdorferi* cyclic-di-GMP-binding protein PlzA reveals a role in motility and virulence. *Infect. Immun.* 79:1815–25
76. Porter SL, Wadhams GH, Armitage JP. 2011. Signal processing in complex chemotaxis pathways. *Nat. Rev. Microbiol.* 9:153–65
77. Raddi G, Morado DR, Yan J, Haake DA, Yang XF, Liu J. 2012. Three-dimensional structures of pathogenic and saprophytic *Leptospira* species revealed by cryo-electron tomography. *J. Bacteriol.*194:1299–306
78. Rao CV, Glekas GD, Ordal GW. 2008. The three adaptation systems of *Bacillus subtilis* chemotaxis. *Trends Microbiol.* 16:480–87
79. Revel AT, Talaat AM, Norgard MV. 2002. DNA microarray analysis of differential gene expression in *Borrelia burgdorferi*, the Lyme disease spirochete. *Proc. Natl. Acad. Sci. USA* 99:1562–67
80. Romeo T. 1998. Global regulation by the small RNA-binding protein CsrA and the non-coding RNA molecule CsrB. *Mol. Microbiol.* 29:1321–30
81. Rosa PA, Tilly K, Stewart PE. 2005. The burgeoning molecular genetics of the Lyme disease spirochaete. *Nat. Rev. Microbiol.* 3:129–43
82. Rosey EL, Kennedy MJ, Yancey RJ Jr. 1996. Dual *flaA1 flaB1* mutant of *Serpulina hyodysenteriae* expressing periplasmic flagella is severely attenuated in a murine model of swine dysentery. *Infect. Immun.* 64:4154–62
83. Ryjenkov DA, Tarutina M, Moskvin OV, Gomelsky M. 2005. Cyclic diguanylate is a ubiquitous signaling molecule in bacteria: insights into biochemistry of the GGDEF protein domain. *J. Bacteriol.* 187:1792–98
84. Sal MS, Li C, Motalab MA, Shibata S, Aizawa S, Charon NW. 2008. *Borrelia burgdorferi* uniquely regulates its motility genes and has an intricate flagellar hook-basal body structure. *J. Bacteriol.* 190:1912–21
85. Samatey FA, Matsunami H, Imada K, Nagashima S, Shaikh TR, et al. 2004. Structure of the bacterial flagellar hook and implication for the molecular universal joint mechanism. *Nature* 431:1062–68
86. Samuels DS, Radolf JD, eds. 2010. *Borrelia: Molecular Biology, Host Interaction and Pathogenesis*. Norfolk, UK: Calister Acad. 548 pp.
87. Shih CM, Chao LL, Yu CP. 2002. Chemotactic migration of the Lyme disease spirochete (*Borrelia burgdorferi*) to salivary gland extracts of vector ticks. *Am. J. Trop. Med. Hyg.* 66:616–21
88. Sourjik V, Armitage JP. 2010. Spatial organization in bacterial chemotaxis. *EMBO J.* 29:2724–33
89. Stanek G, Wormser GP, Gray J, Strle F. 2011. Lyme borreliosis. *Lancet* 379:461–73
90. Sultan SZ, Pitzer JE, Boquoi T, Hobbs G, Miller MR, Motaleb MA. 2011. Analysis of the HD-GYP domain cyclic dimeric GMP phosphodiesterase reveals a role in motility and the enzootic life cycle of *Borrelia burgdorferi*. *Infect. Immun.* 79:3273–83
91. Sultan SZ, Pitzer JE, Miller MR, Motaleb MA. 2010. Analysis of a *Borrelia burgdorferi* phosphodiesterase demonstrates a role for cyclic-di-guanosine monophosphate in motility and virulence. *Mol. Microbiol.* 77:128–42
92. Sze CW, Li C. 2011. Inactivation of *bb0184*, which encodes carbon storage regulator A, represses the infectivity of *Borrelia burgdorferi*. *Infect. Immun.* 79:1270–79
93. Sze CW, Morado DR, Liu J, Charon NW, Xu H, Li C. 2011. Carbon storage regulator A ($CsrA_{Bb}$) is a repressor of *Borrelia burgdorferi* flagellin protein FlaB. *Mol. Microbiol.* 82:851–64
94. Sze CW, Zhang K, Kariu T, Pal U, Li C. 2012. *Borrelia burgdorferi* needs chemotaxis to establish infection in mammals and to accomplish its enzootic cycle. *Infect. Immun.* 80:2485–92

76. Reviews chemotaxis in different species of bacteria.

81. Discusses how recent breakthroughs in the molecular genetics of *Bb* are leading to a better understanding of the pathogenesis of Lyme disease.

86. Gives a comprehensive analysis of the biology of *Bb* and Lyme disease.

95. Thomas DR, Francis NR, Xu C, DeRosier DJ. 2006. The three-dimensional structure of the flagellar rotor from a clockwise-locked mutant of *Salmonella enterica* serovar Typhimurium. *J. Bacteriol.* 188:7039–48
96. Tokarz R, Anderton JM, Katona LI, Benach JL. 2004. Combined effects of blood and temperature shift on *Borrelia burgdorferi* gene expression as determined by whole genome DNA array. *Infect. Immun.* 72:5419–32
97. Turner L, Ryu WS, Berg HC. 2000. Real-time imaging of fluorescent flagellar filaments. *J. Bacteriol.* 182:2793–801
98. Vaknin A, Berg HC. 2004. Single-cell FRET imaging of phosphatase activity in the *Escherichia coli* chemotaxis system. *Proc. Natl. Acad. Sci. USA* 101:17072–77
99. Wadhams GH, Armitage JP. 2004. Making sense of it all: bacterial chemotaxis. *Nat. Rev. Mol. Cell Biol.* 5:1024–37
100. Wei BL, Brun-Zinkernagel AM, Simecka JW, Pruss BM, Babitzke P, Romeo T. 2001. Positive regulation of motility and *flhDC* expression by the RNA-binding protein CsrA of *Escherichia coli*. *Mol. Microbiol.* 40:245–56
101. Weibull C. 1960. Movement. In *The Bacteria, A Treatise on Structure and Function*, ed. IC Gunsalas, RY Stanier, 1:153–234. New York/ London: Academic
102. Wolgemuth CW, Charon NW, Goldstein SF, Goldstein RE. 2006. The flagellar cytoskeleton of the spirochetes. *J. Mol. Microbiol. Biotechnol.* 11:221–27
103. Wuichet K, Zhulin IB. 2010. Origins and diversification of a complex signal transduction system in prokaryotes. *Sci. Signal.* 3:ra50
104. Xu H, Caimano MJ, Lin T, He M, Radolf JD, et al. 2010. Role of acetyl-phosphate in activation of the Rrp2-RpoN-RpoS pathway in *Borrelia burgdorferi*. *PLoS. Pathog.* 6:e1001104
105. Xu H, Raddi G, Liu J, Charon NW, Li C. 2011. Chemoreceptors and flagellar motors are subterminally located in close proximity at the two cell poles in spirochetes. *J. Bacteriol.* 193:2652–56
106. Yakhnin H, Pandit P, Petty TJ, Baker CS, Romeo T, Babitzke P. 2007. CsrA of *Bacillus subtilis* regulates translation initiation of the gene encoding the flagellin protein (*hag*) by blocking ribosome binding. *Mol. Microbiol.* 64:1605–20
107. Yang J, Huber G, Wolgemuth CW. 2012. Forces and torques on rotating spirochete flagella. *Phys. Rev. Lett.* 107:268101
108. Yang X, Goldberg MS, Popova TG, Schoeler GB, Wikel SK, et al. 2000. Interdependence of environmental factors influencing reciprocal patterns of gene expression in virulent *Borrelia burgdorferi*. *Mol. Microbiol.* 37:1470–79
109. Young GM, Badger JL, Miller VL. 2000. Motility is required to initiate host cell invasion by *Yersinia enterocolitica*. *Infect. Immun.* 68:4323–26
110. Yuri K, Takamoto Y, Okada M, Hiramune T, Kikuchi N, Yanagawa R. 1993. Chemotaxis of leptospires to hemoglobin in relation to virulence. *Infect. Immun.* 61:2270–72

103. Provides an extensive genomic analysis of the evolution of chemotaxis genes in bacteria.

105. Uses light microscopy and cryo-EM to analyze one end of a *Bb* cell.

RELATED RESOURCES

Brisson D, Drecktrah D, Eggers CH, Samuels DS. 2012. Genetics of *Borrelia burgdorferi*. *Annu. Rev. Genet.* 46:In press

Hazelbauer GL. 2012. Bacterial chemotaxis: the early years of molecular studies. *Annu. Rev. Microbiol.* 66:285–303

Paul K, Gonzalez-Bonet G, Bilwes AM, Crane BR, Blair D. 2011. Architecture of the flagellar rotor. *EMBO J.* 30:2962–71

Samuels DS. 2011. Gene regulation in *Borrelia burgdorferi*. *Annu. Rev. Microbiol.* 65:479–99

Tilly K, Rosa PA, Stewart PE. 2008. Biology of infection with *Borrelia burgdorferi*. *Infect. Dis. Clin. North Am.* 22:217–34

Annual Review of Microbiology

Volume 66, 2012

Contents

Index

Errata

An online log of corrections to *Annual Review of Microbiology* articles may be found at http://micro.annualreviews.org/